2020 IEEE International Conference on Robotics and Automation (ICRA)
31 May - 31 August, 2020. Paris, France

Nonlinear Vector-Projection Control for Agile Fixed-Wing Unmanned Aerial Vehicles

Juan Carlos Hernández Ramírez[1] and Meyer Nahon[1]

***Abstract*— Agile fixed-wing aircraft integrate the efficient, high-speed capabilities of conventional fixed-wing platforms with the extreme maneuverability of rotorcraft. This work presents a nonlinear control strategy that harnesses these capabilities to enable autonomous flight through aggressive, time-constrained, three-dimensional trajectories. The cascaded control structure consists of two parts; an inner attitude control loop developed on the Special Orthornormal group that avoids singularities commonly associated with other parametrizations, and an outer position control loop that jointly determines the thrust command and attitude references by implementing a novel vector-projection algorithm. The objective of the algorithm is to decouple roll from the reference attitude to ensure that thrust and lift forces can always be pointed such that position errors converge to zero. The proposed control system represents a single, unified solution that remains effective throughout the aircraft's flight envelope, including aerobatic operation. Controller performance is verified through simulations and experimental flight tests; results show the unified control scheme is capable of performing a wide range of operations that would normally require multiple, single-purpose controllers, and their associated switching logic.**

I. INTRODUCTION

Unmanned Aerial Vehicles (UAVs) are increasingly being used for civilian applications, providing solutions for a variety of tasks; as a consequence, research focused on their autonomous operation has expanded in recent years. Fixed-wing UAVs, which generate lift through their wing and other lifting surfaces, are the traditional choice for tasks that require large coverage, endurance, and high-speed flight. However, compared to rotorcraft, their maneuverability is limited: they are incapable of hovering in place, and often require additional infrastructure to take-off and land.

A class of fixed-wing aircraft, equipped with propulsion systems with a large thrust-to-weight ratio, coupled with high aspect ratio wings and large control surfaces that capitalize on propeller slipstream, like the one in Fig. 1, have demonstrated the capacity to perform aggressive, precise aerobatic maneuvers [1]. These platforms, known as agile fixed-wing aircraft, bridge the gap between conventional fixed-wing aircraft and rotorcraft. Their unique design allows them to remain airborne even when the lifting surfaces no longer generate sufficient lift, while retaining control authority through propeller slipstream over the control surfaces. Indeed, the slipstream greatly enhances the motions of agile UAVs as demonstrated in [2]. In order for agile fixed-wing UAVs to be used more broadly, control systems capable of harnessing this increased maneuverability need to be developed.

Fig. 1: McFoamy agile fixed-wing platform

Conventional fixed-wing control systems are not suited for agile fixed-wing platforms due to their design limitations. Both the guidance logic, which restricts the aircraft such that its motions simplify to a Dubins-type kynematics, and the use of Euler angles which are not global, result in an aircraft constrained to a minimum turn radius, a minimum airspeed, a small flight path angle, and limited path shapes [3]. Agile fixed-wing aircraft are not bound by these limitations but few autonomous control strategies that account for this added maneuverability have been developed. In [4] a quaternion based controller is proposed to enable the aircraft to switch between level flight and hover. The work presented in [5] offers a similar solution where the controller switches into hover mode through discontinuous references. In [6], [7] two distinct control strategies are developed for steady and aerobatic flight. By contrast, [8] develops a unified position and attitude tracking controller which allows the UAV to perform a wide range of aerobatic maneuvers while remaining on a path. This control architecture requires matched, dynamically feasible attitude and position references which can be challenging to determine. A different approach is pursued in [1] where the controller manipulates the thrust and aerodynamic forces to generate a desired acceleration that will satisfy a path. Trajectories are easier to build since only position references are required, but the controller requires very precise knowledge on the aircraft aerodynamics in various regimes.

The control system developed in [7] eliminates the need to specify matched attitude references. The present work improves upon this formulation by unifying the control strategy such that it is valid for all regimes. A similar cascaded structure is chosen but the position control loop takes design cues from controllers for thrust-borne aircraft

*This work was supported the McGill Engineering Doctoral Award (MEDA) and the CONACyT grant for studies abroad.

[1]Juan Carlos Hernandez and Meyer Nahon are with the Department of Mechanical Engineering, McGill University, Montreal, QC, Canada.

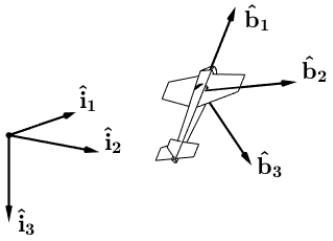

Fig. 2: Inertial and body reference frames

[9], [10] while incorporating a novel projection algorithm to properly account for the generated lift. The main contribution of this work is the development of a novel control system that enables an agile fixed-wing UAV to make use of its highly maneuverable characteristics to follow aggressive, time-parametrized flight paths well beyond the limitations of conventional flight systems. The proposed controller remains valid throughout the aircraft's flight envelope, including steady flight, transitions to and from hover, and aerobatic maneuvering. It does so while using a completely unified control structure, thus avoiding potential instability due to switching behavior and reducing the complexity of controller implementation and tuning. The proposed controller is readily applicable to other platforms such as tailsitters and can be adapted to certain rotorcraft and fixed-wing hybrids.

II. CONTROL SYSTEM

A. Agile Fixed-wing Model

To describe the three-dimensional motion of the aircraft, two reference frames are required. As is common in UAVs, the North-East-Down (NED) convention is adopted such that the $\hat{\mathbf{i}}_1$, $\hat{\mathbf{i}}_2$, $\hat{\mathbf{i}}_3$ basis vectors of the inertial reference frame, $\boldsymbol{\mathcal{F}}_i$, align with the North, East, and Down directions, respectively. Similarly, the body reference frame, $\boldsymbol{\mathcal{F}}_b$ is affixed to aircraft centre of mass, and is selected such that the $\hat{\mathbf{b}}_1$ basis vector points out of the aircraft nose, the $\hat{\mathbf{b}}_2$ vector points out of the starboard wing, and the $\hat{\mathbf{b}}_3$ vector points out of the aircraft belly. These reference frames are shown in Fig. 2.

The equations of motion of the UAV are

$$\dot{\mathbf{p}}_i = \mathbf{C}_{bi}^T \mathbf{v}_b \tag{1}$$

$$m\dot{\mathbf{v}}_b = -\boldsymbol{\omega}_b^{\times} m\mathbf{v}_b + mg\,\mathbf{C}_{bi}\hat{\mathbf{k}}_3 + \mathrm{T}\,\hat{\mathbf{k}}_1 + \mathbf{F}_{aero} + \mathbf{F}_{\delta} \tag{2}$$

$$\dot{\mathbf{C}}_{bi} = -\boldsymbol{\omega}_b^{\times}\mathbf{C}_{bi} \tag{3}$$

$$\mathbf{J}\dot{\boldsymbol{\omega}}_b = (\mathbf{J}\boldsymbol{\omega}_b)^{\times}\boldsymbol{\omega}_b + \mathbf{M}_{\delta} + \mathbf{M}_{aero} + \mathbf{M}_{gyro} \tag{4}$$

where the UAV mass, m, and the second moment of mass, $\mathbf{J}$, are considered constant since the body is considered rigid. The operator $(\cdot)^{\times}$ is the skew symmetric operator as defined in [11]. The unit vectors $\hat{\mathbf{k}}_1 = [1\,0\,0]^T$ and $\hat{\mathbf{k}}_3 = [0\,0\,1]^T$ are defined for simplicity and will be used in the control derivation. The state space is composed by $\mathbf{p}_i$, the position of the centre of mass of the UAV in inertial frame coordinates, $\mathbf{v}_b$, the velocity of the centre of mass resolved in body frame coordinates, $\boldsymbol{\omega}_b$, the angular velocity of the body frame with respect to the inertial frame in body frame coordinates, and $\mathbf{C}_{bi}$, the Direction Cosine Matrix (DCM) from inertial to body frame. The DCM belongs to the Special Orthonormal group, SO(3), and is the natural description of attitude. This representation is used here since it has no singularities and hence is able to represent any attitude the UAV might operate at. This choice also avoids problems associated with other non-singular attitude parametrizations, such as the unwinding phenomenon in quaternion space.

Forces acting upon the UAV are the aircraft's weight, mg, thrust, T, and aerodynamic forces, $\mathbf{F}_{aero}$ mainly composed of lift and drag. Forces due to control surface deflection, also aerodynamic in nature, are represented by $\mathbf{F}_{\delta}$. The aircraft is also subject to a gyroscopic moment, $\mathbf{M}_{gyro}$, and various aerodynamic moments, where a distinction is made between moments that can be directly controlled through the UAV control surfaces, $\mathbf{M}_{\boldsymbol{\delta}}$ and those arising naturally from the aircraft configuration, $\mathbf{M}_{aero}$.

The main goal of the developed control system is to follow a desired a trajectory, prescribed only by a time parametrized inertial position reference and its derivatives, $\mathbf{p}_r(t)$, $\dot{\mathbf{p}}_r(t)$, $\ddot{\mathbf{p}}_r(t)$. This position reference is not limited to a Dubins-type path [12] or a modification thereof [13] but is fully three-dimensional and arbitrarily aggressive. An important feature of the control system is that a matching attitude reference need not be specified; similarly, aerobatic maneuvers don't need to be explicitly prescribed. Rather, the control system will execute an aerobatic maneuver if the constraints of the path demand it. The tracking objective is to drive to zero the the position tracking errors

$$\mathbf{e} = \mathbf{p}_r - \mathbf{p}_i, \qquad \dot{\mathbf{e}} = \dot{\mathbf{p}}_r - \mathbf{C}_{bi}^T\mathbf{v}_b. \tag{5}$$

We use a cascaded control architecture consisting of an inner attitude control loop and an outer position control loop. The outer position control loop determines the reference thrust command and reference attitude that will drive the position errors to zero. The inner attitude tracking control loop then determines the control surface deflections needed to achieve the desired attitude. A key characteristic is that this is a unified control system valid for all maneuvers and regimes. At no point does the aircraft switch between control architectures to operate in different regimes; thrust and reference attitude are always determined continuously through a single algorithm. Moreover, as will be shown, a single set of control gains can be used to accommodate a wide range of flight regimes.

B. Attitude Controller

The attitude control is based on the same structure as the one employed in [10], but adapted for use on a fixed-wing aircraft. Consider first an arbitrary time-evolving attitude profile prescribed through a reference kinematic equation:

$$\dot{\mathbf{C}}_{ri} = -\boldsymbol{\omega}_r^{\times}\mathbf{C}_{ri}, \qquad \mathbf{e}_{att} = \boldsymbol{\mathcal{P}}_a(\mathbf{C}_{br})^{\vee}, \tag{6}$$

where $\mathbf{C}_{br} = \mathbf{C}_{bi}\mathbf{C}_{ri}^T$ is the error DCM, the anti-symmetric projection operator on square matrices $\boldsymbol{\mathcal{P}}_a(\cdot)$ is defined as $\boldsymbol{\mathcal{P}}_a(\mathbf{A}) = \frac{1}{2}(\mathbf{A} - \mathbf{A}^T)$ and $(\cdot)^{\vee}$ is the uncross operator which operates on skew-symmetric matrices, such that $(\mathbf{x}^{\times})^{\vee} = \mathbf{x}$.

To drive the attitude errors to zero, a nonlinear PD control

law is proposed as

$$\mathbf{M}_\delta = -\mathbf{K}_{ad}(\boldsymbol{\omega} - \mathbf{C}_{br}\boldsymbol{\omega}_r) + \mathbf{K}_{ap}\mathbf{e}_{att} \tag{7}$$

where $\mathbf{K}_{ap} = \mathbf{K}_{ap}^T > 0$ and $\mathbf{K}_{ad} = \mathbf{K}_{ad}^T > 0$ are the attitude control gains.

Moments need to be translated into control surface deflections which inevitably requires some knowledge on the aircraft aerodynamics. Following [7], a simplified model based on control surface coefficients is used. Consider the mapping between control surface deflections and moments

$$\delta_{aileron} = \frac{M_{\delta_1}}{0.5\rho V_s^2 S b C_{\delta_a}} \tag{8}$$

$$\delta_{elevator} = \frac{M_{\delta_2}}{0.5\rho V_s^2 S \bar{c} C_{\delta_e}} \tag{9}$$

$$\delta_{rudder} = \frac{M_{\delta_3}}{0.5\rho V_s^2 S b C_{\delta_r}} \tag{10}$$

where ρ is the air density, b, $\bar{c}$, and S are the aircraft parameters of wing span, mean chord, and wing area, respectively, C_{δ_a}, C_{δ_e}, and C_{δ_r} are the control surface coefficients for aileron, elevator, and rudder, and V_s is the airspeed over the control surfaces which is approximated using momentum theory [14], [8] to account for slipstream through

$$V_s = 0.5\left(v_{b_1} + \sqrt{v_{b_1}^2 + 4\mathrm{T}/(\rho\pi R^2)}\right), \tag{11}$$

where R is the propeller radius. Due to the propeller slipstream, the airflow over the control surfaces is non-zero even when the aircraft is hovering. The mapping between control surface deflections and moments allows the use of known aircraft aerodynamics to adjust the control deflections as the airflow over the control surfaces changes. Since the attitude control gain matrices always remain positive definite, imprecise knowledge does not result in instability, though the tracking performance might be diminished.

C. Position Control

Compared to conventional fixed-wing platforms, thrust is a significant force in all regimes; much more so in maneuvers when the wing has stalled. The control system is initially developed around regimes where thrust is particularly dominant and the aircraft is essentially thrust-borne.

Consider the translational dynamic equation, but derived in the inertial frame

$$\dot{\mathbf{v}}_i = \ddot{\mathbf{p}}_i = g\hat{\mathbf{k}}_3 + \frac{\mathrm{T}}{m}\mathbf{C}_{bi}^T\hat{\mathbf{k}}_1 \tag{12}$$

where the assumption has been made that for maneuvers close to hover, the aerodynamic forces are much smaller compared to thrust. This assumption is reasonable given the high angle of attack and the reduced airspeed. The equation is similar to the description of rotorcraft and, indeed, this approach is inspired by position tracking strategies developed for those platforms. Analogous to [9], suppose that given some $\mathbf{F} \in \mathcal{R}^3$ a combination of thrust and reference attitude exist such that

$$\frac{\mathrm{T}}{m}\mathbf{C}_{ri}^T\hat{\mathbf{k}}_1 = \mathbf{F} \tag{13}$$

where $\mathbf{C}_{ri}$ is the DCM associated with the reference attitude required by the attitude controller. Substituting (13) in (12) results in

$$\dot{\mathbf{v}}_i = g\hat{\mathbf{k}}_3 + \mathbf{F} - \frac{\mathrm{T}}{m}\left(\mathbf{C}_{ri} - \mathbf{C}_{bi}\right)^T\hat{\mathbf{k}}_1.$$

Define a control law in terms of the errors (5) by assigning to the intermediate command, $\mathbf{F}$:

$$\mathbf{F} = \ddot{\mathbf{p}}_r + \mathbf{K}_{td}\dot{\mathbf{e}} + \mathbf{K}_{tp}\mathbf{e} - g\hat{\mathbf{k}}_3 \tag{14}$$

with $\mathbf{K}_{td} = \mathbf{K}_{td}^T > 0$ and $\mathbf{K}_{tp} = \mathbf{K}_{tp}^T > 0$. When substituted in the position dynamics it results in the error dynamics,

$$\ddot{\mathbf{e}} + \mathbf{K}_{td}\dot{\mathbf{e}} + \mathbf{K}_{tp}\mathbf{e} = \frac{\mathrm{T}}{m}\left(\mathbf{C}_{bi} - \mathbf{C}_{ri}\right)^T\hat{\mathbf{k}}_1.$$

The right-hand term can be considered a perturbation due to the UAV attitude not converging instantly to the reference one required to generate (14). The nominal error dynamics, without this perturbation, represent a stable, linear system which is exponentially stable with respect to the origin. Due to the inner attitude controller, the perturbation term vanishes at a faster rate than the evolution of the slower translational dynamics so overall stability is preserved [15].

D. Vector Projection Algorithm

The command (14) must be produced through a coordinated selection of thrust, T, and reference attitude, $\mathbf{C}_{ri}$, through (13). One solution is to set the thrust as

$$\mathrm{T} = m\|\mathbf{F}\|, \tag{15}$$

which, when substituted in (13), results in

$$\hat{\mathbf{f}} \triangleq \frac{\mathbf{F}}{\|\mathbf{F}\|} = \mathbf{C}_{ri}^T\hat{\mathbf{k}}_1. \tag{16}$$

The attitude determination problem is now equivalent to Wahba's problem with one constraint: the thrust vector (aircraft nose), $\hat{\mathbf{k}}_1$ must align with $\hat{\mathbf{f}}$. This problem itself has infinitely many solutions and the method selected has a large impact on the resulting aircraft behavior. In both [9], [16] the reference attitudes are selected to ensure the shortest possible rotation. This is sufficient for a multirotor but is not ideal for a fixed-wing aircraft where aerodynamic forces are not only significant, but fundamental to its operation. The attitude determination problem is incomplete in the sense that rotation around the thrust axis is not specified, this corresponds to the roll angle in fixed-wing aircraft and it determines how lift is directed. If roll is to be prescribed independently, the baseline reference attitude must decouple roll. In other words, to allow for a sequential operation to correctly prescribe the motion around the thrust axis, the baseline reference attitude must guarantee zero roll. Ideally, this condition should be specified without any Euler angle decomposition that would reintroduce singularities to the control system.

An analogous problem was explored in [17] where the reference attitude also needed to verify two conditions. The algorithm developed here is a heavily modified version of the solution presented there, applied in this work to resolve

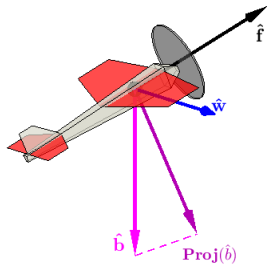

Fig. 3: Downwards projection algorithm

the roll decoupling problem. The proposed reference attitude determination problem is formulated as follows. Find $\mathbf{C}_{ri}$ such that $\hat{\mathbf{k}}_1$ aligns with $\hat{\mathbf{f}}$ while keeping the aircraft belly vector, $\hat{\mathbf{k}}_3$ as close as possible to the downwards pointing vector, $\hat{\mathbf{b}} = [0\,0\,1]^T$. A vector projection algorithm can be used to achieve this. Compute a vector normal to the two conditions through

$$\mathbf{W} = \hat{\mathbf{b}} \times \hat{\mathbf{f}}. \tag{17}$$

This new vector, $\mathbf{W}$, is not necessarily unit norm, since

$$\|\mathbf{W}\| = \|\hat{\mathbf{b}}\|\|\hat{\mathbf{f}}\| \sin\theta = \sin\theta$$

where θ is the angle between both vectors. Normalizing,

$$\hat{\mathbf{w}} = \frac{\mathbf{W}}{\|\mathbf{W}\|}. \tag{18}$$

The belly vector closest to the downward direction is the projection of $\hat{\mathbf{b}}$ normal to the plane created by $\hat{\mathbf{w}}$ and $\hat{\mathbf{f}}$,

$$\text{Proj}(\hat{\mathbf{b}}) = \hat{\mathbf{f}} \times \hat{\mathbf{w}}. \tag{19}$$

The three vectors $\hat{\mathbf{f}}$, $\hat{\mathbf{w}}$, and $\text{Proj}(\hat{\mathbf{b}})$ are orthonormal and obey the right-hand rule. Aligning the aircraft's three body axes with these vectors ensures the aircraft will point its thrust to achieve the position control objective, while pointing its belly as downwards as possible. This second condition has as consequence that the vector associated with the direction of the wing, $\hat{\mathbf{w}}$ is always contained in the North-East plane. This situation is shown in Fig. 3.

Finally, it is straightforward to show that the reference attitude can be expressed as

$$\mathbf{C}_{ri} = \begin{bmatrix}\hat{\mathbf{f}} & \hat{\mathbf{w}} & \text{Proj}(\hat{\mathbf{b}})\end{bmatrix}^T. \tag{20}$$

E. Geometric singularity during hover

The projection algorithm encounters a singularity when $\hat{\mathbf{f}}$ and $\hat{\mathbf{b}}$ become parallel. This will create a problem in (18), since the norm tends to zero. This is a geometric singularity and obeys a clear physical impediment: the aircraft cannot point the nose upwards (or downwards) while pointing the belly downwards. This can be avoided by relaxing the projection condition when the aircraft is sufficiently pitched upwards. To obtain an attitude reference, one solution is to *lock* the wing in position. This can be accomplished through building the DCM differently.

If the angle between vectors is deemed too small, or, alternatively, the reference velocity in the NE plane is too slow, calculate the reference attitude as follows. The auxiliary vector is defined as

$$\hat{\mathbf{a}} = \frac{\hat{\mathbf{f}} \times \hat{\mathbf{w}}_p}{\|\hat{\mathbf{f}} \times \hat{\mathbf{w}}_p\|} \tag{21}$$

where $\hat{\mathbf{w}}_p$ is the projection onto the NE plane of the last, previously calculated $\hat{\mathbf{w}}$ vector. Through this definition, $\hat{\mathbf{a}}$ will be arbitrarily close to the previous projection of the downwards vector. Next, calculate the new wing vector as the projection of the previous wing vector

$$\text{Proj}(\hat{\mathbf{w}}_p) = \hat{\mathbf{a}} \times \hat{\mathbf{f}} \tag{22}$$

Finally, the reference DCM is built as

$$\mathbf{C}_{ri} = \begin{bmatrix}\hat{\mathbf{f}} & \text{Proj}(\hat{\mathbf{w}}_p) & \hat{\mathbf{a}}\end{bmatrix}^T \tag{23}$$

This solution keeps the thrust direction continuous, while keeping the overall reference attitude with little to no discontinuities. The thrust magnitude is calculated through the same algorithm and hence remains continuous as well.

F. Roll augmentation

This new algorithm guarantees that the reference attitude, if parametrized using Euler angles, will possess zero roll, irrespective of the orientation of the thrust direction vector. On its own, this already guarantees a much smoother operation, since the wing is level. The main benefit of this solution, however, is that any motion around the thrust axis can now be independently prescribed while still satisfying (13). Since the rotation around this axis effectively allows the aircraft to direct the lift generated by its main lifting surface, this decoupling is a fundamental feature.

For fully autonomous operation, a bank can be introduced through a guidance algorithm in order to reduce the cross track error, akin to [12]. Calculate the UAV course and reference course as

$$\chi = \text{atan2}(v_{i_2}, v_{i_1}), \tag{24}$$

$$\chi_r = \text{atan2}(\dot{p}_{r_2}, \dot{p}_{r_1}). \tag{25}$$

The cross track error is then defined as

$$y_e = -\sin(\chi)e_1 + \cos(\chi)e_2, \tag{26}$$

and the adjusted course error and the reference roll are computed through

$$\chi_e = \chi_r - \chi + \text{atan}(k_y\, y_e), \tag{27}$$

$$\phi_r = k_\chi \chi_e, \tag{28}$$

with $k_y, k_\chi > 0$. Finally, the roll-augmented reference attitude can be calculated through a sequential change of reference frame:

$$\bar{\mathbf{C}}_{ri} = \begin{bmatrix}1 & 0 & 0\\ 0 & \cos(\phi_r) & \sin(\phi_r)\\ 0 & -\sin(\phi_r) & \cos(\phi_r)\end{bmatrix}\mathbf{C}_{ri} \tag{29}$$

G. Controller properties

The proposed control system has a number of desirable properties. From the system theory perspective, the single, control system avoids sudden switching which could induce

instabilities. The all-in-one structure makes implementation simpler: the attitude controller can be tuned independently with external attitude references while the position PID position control gains can be independently selected for each coordinate. Other linear control techniques can be used to define (14), such as optimal or robust approaches.

The attitude determination algorithm enforces an additional attitude constraint without need of attitude measurements or any Euler angle decomposition. This enables the position loop to operate with only inertial position and velocity measurements as feedback.

From the aircraft control perspective, the proposed control system also has a number of advantageous features. In the steady flight regime, the control system essentially operates as a set of standard longitudinal and lateral autopilots, but enhanced to operate for more complex 3D maneuvers. Additionally, the control system naturally uses the rudder to perform a coordinated banked turn without the need of overparametrizing heading or heading rate. Finally, the thrust is always positive by design; unlike conventional PID schemes, there is no need to prescribe a lower bound and no realistic mode of operation will drive the commanded thrust to zero.

III. SIMULATION AND EXPERIMENTS

The designed control system was first evaluated through non-real-time numerical simulations, followed by Software-in-the-Loop (SITL) simulations. The high-fidelity model of our agile fixed-wing UAV accounts for the full operating envelope of the aircraft. It is based on the aerodynamic analysis presented in [18], with a thruster model accounting for multiple flow characteristics [19], and a slipstream model to simulate this key feature of agile UAVs [14]. The SITL simulation was used to refine and evaluate the control structure, as well as to determine initial control gains. It allowed this process to take place in a safe laboratory environment, rather than risking damage to the physical platform at this precarious stage of development. Following this, experimental tests were undertaken to further adjust the control gains, as needed. The position control gains required minimal adjustment from those in the SITL, while the attitude control gains had to be reduced to compensate for the effects of sensor noise. The final values of the experimental gains, kept constant throughout all the field trial maneuvers discussed next, are given in Table I.

An off-the-shelf WM Parkflyers McFoamy RC aircraft, shown in Fig. 1, with mass of 0.45 kg and 0.86 m wingspan was employed for the field trials. Other aircraft properties can be found in [8], [7]. The control algorithm was implemented within the Pixracer embedded autopilot hardware. This system uses a 180 MHz ARM Cortex M4 processor and runs Px4 software allowing for attitude and angular velocity estimation with built-in sensors, and position and velocity estimates when augmented with a GPS unit. The experiments were conducted outdoors with a mean wind of about 15 km/h at an angle between 100° and 140° from true north, with gusts up to 30 km/h.

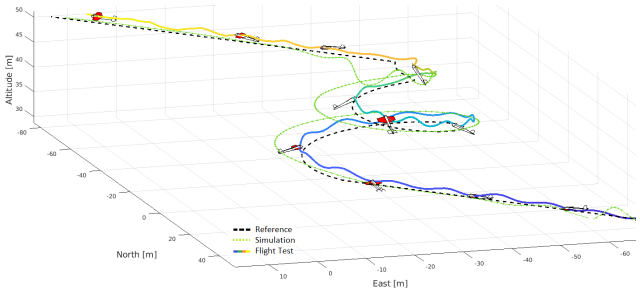

Fig. 4: Simulation and experimental results for climbing spiral maneuver

TABLE I:
Controller gains

Gain	Value
$\mathbf{K}_{ad}$	diag(0.00706,0.07576, 0.07736)
$\mathbf{K}_{ap}$	diag(0.1656, 1.022, 0.6776)
$\mathbf{K}_{td}$	diag(0.21, 0.21, 0.11)
$\mathbf{K}_{tp}$	diag(0.54, 0.54, 0.72)
k_χ	0.216
k_y	0.08

A series of different flight paths were commanded for the aircraft to track. For all simulations and experiments, the reference attitude with the augmented roll (29) was used. A climbing spiral maneuver was designed to showcase the capabilities of the control algorithm. The SITL and the experimental flight paths of this maneuver are shown in Fig. 4. The corresponding position and attitude plots of this experimental flight are given in Figs. 5 and 6, respectively.

The aircraft is first commanded to follow a straight line at a heading of 138° at 15 m/s while holding altitude, which is typical of steady level flight. After five seconds, the aircraft enters a climbing tightening spiral with an initial radius of 20 m and 1 m/s climb rate. The velocity at the entry to the spiral is discontinuous which requires the aircraft to suddenly decelerate to 12.5 m/s, achieved through a combination of pitching motions and thrust adjustments. The radius continuously contracts at a rate of 1 m/s and the velocity correspondingly decreases. Eventually, the velocity of the reference has decreased such that the aircraft has become thrust-borne. At the peak of the maneuver, 20 seconds after initiating the spiral, the reference velocity is zero and the aircraft hovers in place briefly. Finally, the aircraft is suddenly commanded to transition back into steady flight at the same initial heading (138°). While the experimental conditions included significant wind disturbances, these were not included in the SITL, since their timing and strength was unknown from available measurements.

Fig. 5 shows the tracking performance of the UAV. Control gains prioritize altitude and indeed the aircraft does a good job of following this reference. The greater control gains, coupled with a less accurate position and velocity estimates in this coordinate does result in oscillations, which can be reduced with further tuning of the control gains. In contrast, the tracking in the horizontal plane is mainly corrupted by external disturbances: wind gusts. The UAV is a light-weight

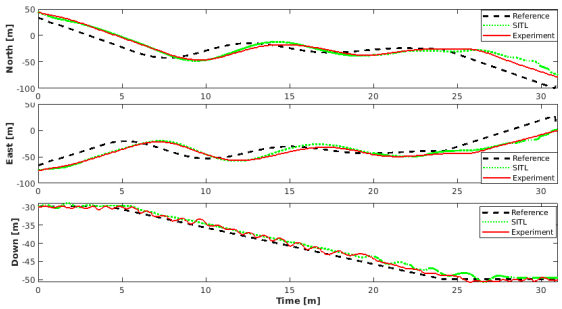

Fig. 5: Experimental results: Position

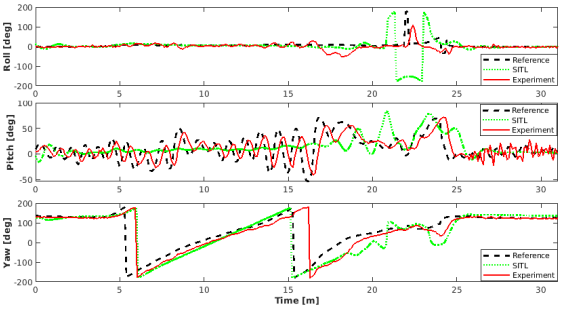

Fig. 6: Experimental results: Attitude

platform, and is thus very susceptible to wind. In Fig. 4 we note that the aircraft drifts in the direction of the wind, but the control system keeps the aircraft close to the reference path, and does so in a time constrained manner as can be appreciated in Figs. 5 and 6. We also note that the SITL results are generally smoother than the experimental flight since they do not consider any wind, but they do show a good overall match to the experimental results.

For additional analysis, the aircraft's attitude is shown as Euler angles in Fig. 6. The reference attitude is completely internal to the control system and the plots showcase the complex, aggressive maneuvering required to allow the aircraft to track the reference trajectory while in the presence of disturbances. This plot makes apparent the difficulty in specifying matched attitude and position profiles, if that were required by the controller. Moreover, even if a nominal attitude profile could be determined, it would likely not be robust in the presence of disturbances. In the present conditions, the control system opted for yawing motions as opposed to more intuitive banking. A separate experiment was conducted with a manually pre-computed roll profile that nominally achieves the required heading rate but was found to perform poorly under windy conditions (not shown here). SITL attitude measurements appear to show discontinuous changes in roll but this is due to the built-in attitude transformation functions in the simulation software.

Two other maneuvers are briefly presented to demonstrate the capabilities of the control system. Fig. 7 shows the trajectory for an aggressive, 150° change in heading. Since the aircraft is following a time parametrized trajectory, it reacts as soon as the reference creates errors, without waiting to complete its initial path to change directions.

Finally, Fig. 8 shows the results for 90° climb maneuver at a climb rate of 5 m/s. Due to the presence of wind,

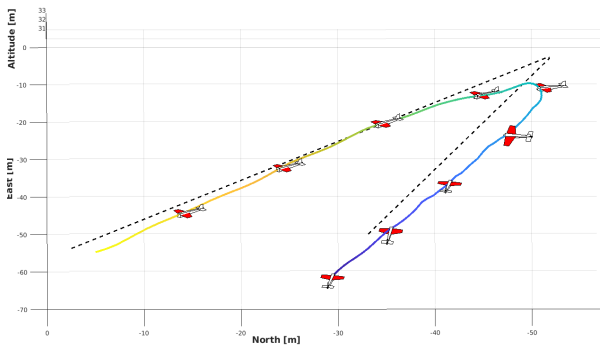

Fig. 7: Experimental results for aggressive change in heading

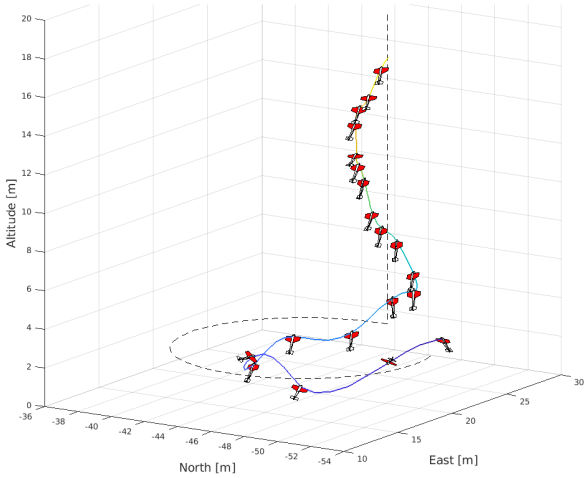

Fig. 8: Experimental results for vertical climb

the aircraft oscillates around the north-east reference but manages to remain close to the path while achieving the required climb rate. A noteworthy aspect of this maneuver is that the roll angle becomes locked in place as designed to avoid the singularity.

IV. CONCLUSIONS

This work presents a novel control system to enable agile fixed-wing UAVs to track aggressive, non-conventional trajectories. The controller represents an unified solution for a wide array of fixed-wing control challenges while boasting several desirable properties ranging from its use of continuous signals to its comparative ease of implementation. Numerical simulations and experimental flight results verify the theoretical properties of the developed system. The experiments demonstrate that the single control structure allows the aircraft to perform a series of aggressive maneuvers which require transitioning between steady and non-steady regimes at different intervals. Furthermore, trajectory generation is simplified as only position references are required with no prior knowledge of which flight regime is required by the UAV to track them.

Future work will focus on studying different control techniques on both control loops to increase robustness to external disturbances encountered in outdoors operations, as well as adapting the present work in order to develop a highly maneuverable, pilot-assist control system.

REFERENCES

[1] S. Park, "Autonomous aerobatics on commanded path," *Aerospace Science and Technology*, vol. 22, no. 1, pp. 64–74, 2012.

[2] J. M. Levin, A. A. Paranjape, and M. Nahon, "Sideslip and slipstream in extreme maneuvering with fixed-wing unmanned aerial vehicles," *Journal of Guidance, Control, and Dynamics*, vol. 41, no. 7, pp. 1610–1616, 2018.

[3] R. W. Beard and T. W. McLain, *Small unmanned aircraft: Theory and practice*. Princeton university press, 2012.

[4] W. E. Green and P. Y. Oh, "A hybrid mav for ingress and egress of urban environments," *IEEE Transactions on Robotics*, vol. 25, no. 2, pp. 253–263, 2009.

[5] A. Frank, J. McGrew, M. Valenti, D. Levine, and J. How, "Hover, transition, and level flight control design for a single-propeller indoor airplane," in *AIAA Guidance, Navigation and Control Conference and Exhibit*, p. 6318, 2007.

[6] F. M. Sobolic, *Agile flight control techniques for a fixed-wing aircraft*. PhD thesis, Massachusetts Institute of Technology, 2009.

[7] J. C. Hernandez Ramirez and M. Nahon, "Trajectory tracking control of highly maneuverable fixed-wing unmanned aerial vehicles," in *AIAA Scitech 2020 Forum*, p. 2074, 2020.

[8] E. Bulka and M. Nahon, "Autonomous control of agile fixed-wing uavs performing aerobatic maneuvers," in *2017 international conference on unmanned aircraft systems (ICUAS)*, pp. 104–113, IEEE, 2017.

[9] A. Roberts and A. Tayebi, "Adaptive position tracking of vtol uavs," *IEEE Transactions on Robotics*, vol. 27, no. 1, pp. 129–142, 2010.

[10] T. Lee, "Geometric tracking control of the attitude dynamics of a rigid body on so (3)," in *Proceedings of the 2011 American Control Conference*, pp. 1200–1205, IEEE, 2011.

[11] J.-Y. Wen and K. Kreutz-Delgado, "The attitude control problem," *IEEE Transactions on Automatic control*, vol. 36, no. 10, pp. 1148–1162, 1991.

[12] E. Oland and R. Kristiansen, "Quaternion-based backstepping control of a fixed-wing unmanned aerial vehicle," in *2013 IEEE Aerospace Conference*, pp. 1–7, IEEE, 2013.

[13] A. Bry, C. Richter, A. Bachrach, and N. Roy, "Aggressive flight of fixed-wing and quadrotor aircraft in dense indoor environments," *The International Journal of Robotics Research*, vol. 34, no. 7, pp. 969–1002, 2015.

[14] W. Khan and M. Nahon, "Development and validation of a propeller slipstream model for unmanned aerial vehicles," *Journal of Aircraft*, vol. 52, no. 6, pp. 1985–1994, 2015.

[15] H. J. Marquez, *Nonlinear control systems: analysis and design*, vol. 1. Wiley-Interscience Hoboken, 2003.

[16] Y. Zou, "Trajectory tracking controller for quadrotors without velocity and angular velocity measurements," *IET Control Theory & Applications*, vol. 11, no. 1, pp. 101–109, 2016.

[17] T. Lee, M. Leok, and N. H. McClamroch, "Geometric tracking control of a quadrotor uav on se (3)," in *49th IEEE conference on decision and control (CDC)*, pp. 5420–5425, IEEE, 2010.

[18] W. Khan and M. Nahon, "Real-time modeling of agile fixed-wing uav aerodynamics," in *2015 international conference on unmanned aircraft systems (ICUAS)*, pp. 1188–1195, IEEE, 2015.

[19] W. Khan and M. Nahon, "Toward an accurate physics-based uav thruster model," *IEEE/ASME Transactions on Mechatronics*, vol. 18, no. 4, pp. 1269–1279, 2013.